



# CHORUS

This is the accepted manuscript made available via CHORUS. The article has been published as:

## Directional short range order in $L1_{\{0\}}$ FeMnPt magnetic thin films

Cheng-Jun Sun, Dongbin Xu, Steve M. Heald, Jingsheng Chen, and Gan-Moog Chow  
Phys. Rev. B **84**, 140408 — Published 18 October 2011

DOI: [10.1103/PhysRevB.84.140408](https://doi.org/10.1103/PhysRevB.84.140408)

# Directional short range order in $L1_0$ FeMnPt magnetic thin films

Cheng-Jun Sun,<sup>1\*</sup> Dongbin Xu,<sup>1,2</sup> Steve M. Heald,<sup>1</sup> Jingsheng Chen,<sup>2</sup> and  
Gan-Moog Chow<sup>2†</sup>

1. Advanced Photon Source, Argonne National Laboratory, Argonne, IL 60439

2. Department of Materials Science and Engineering, National University of  
Singapore, Singapore 117576

\*To whom correspondence should be addressed. [cjsun@aps.anl.gov](mailto:cjsun@aps.anl.gov)

†To whom correspondence should be addressed. [msecgm@nus.edu.sg](mailto:msecgm@nus.edu.sg)

A new method for investigating the directional short range order (DSRO) of an element of interest in  $L1_0$  FeMnPt thin films using polarization dependent x-ray absorption near edge structure (XANES) spectroscopy is described. The XANES calculations for both  $L1_0$  FePt and  $L1_0$  MnPt phases indicate that the height of the low energy shoulder of the polarization dependent XANES is proportional to the degree of DSRO of the element of interest in case of  $L1_0$  FePt and MnPt systems. The experimentally observed DSRO of Fe and Mn in  $L1_0$  FeMnPt magnetic thin films are consistent with a decrease of ordering parameter with increasing Mn doping. We demonstrate theoretically and experimentally that the heights of the low energy shoulder in the Fe K- and Mn K- edge polarization dependent XANES are proportional to the DSRO of Fe and Mn, respectively.

PACS numbers: 61.05.cj, 75.40.-s, 75.70.Ak, 78.40.Kc,

The properties of magnetic thin films depend on both long-range order (LRO) and short-range order (SRO) especially the directional short-range order (DSRO) [1], which is the SRO in a specific lattice direction. The strong spin-lattice interaction in magnetic materials often leads to either alignment or anti-alignment of the neighboring spins, thus giving rise to ferromagnetic (FM) or antiferromagnetic (AFM) phases [2]. The role of DSRO such as the elemental specific coordination number at a given lattice direction is essential to understand the complexity of the antiferromagnetism and ferromagnetism in a system with the coexistence of AFM and FM phases. In particular, one would expect that a change in the magnetic properties could be quite dramatic when the DSRO is changed [3].

A model system for this study is the  $L1_0$  FeMnPt phase, which is famously known for the coexistence of the  $L1_0$  FM FePt and  $L1_0$  AFM MnPt phases [4]. The magnetic and electronic properties with models of various spin configurations in  $L1_0$  ordered MnPt and FePt alloys were investigated theoretically using first-principles theory [5]. The relative energies with respect to that of the most stable magnetic moment direction for a give model are compared, as shown in Fig. 1. It has been theoretically demonstrated that the most stable phase of  $L1_0$  MnPt is AFM with all the spins within the (001) plane [5] aligning in an alternating chessboard arrangement and with a FM spin arrangement between adjacent (001) planes. In contrast,  $L1_0$  FePt is a FM phase with the stable status of all spins aligning perpendicular to the (001) direction. In this study, the DSRO of Fe and Mn is defined as the fraction of Fe-Fe bonds and Mn-Mn bonds in a given lattice plane or direction. Therefore, the fraction of AFM phase or (and) FM phase in  $L1_0$  FeMnPt is associated to

the DSRO of Fe and Mn both parallel and perpendicular to the (001) plane. However, little is known about the DSRO in  $L1_0$  FeMnPt (001) magnetic thin films from either theoretical or experimental points of view.

DSRO has been previously investigated using polarization dependent extended x-ray absorption fine structure (EXAFS) [6,7]. However, EXAFS is not an appropriate tool for investigating materials consisting of elements with similar lattice parameters, backscattering amplitudes, and phase shifts [8], such as Mn and Fe. In this study, we demonstrate theoretically and experimentally that in  $L1_0$  FeMnPt magnetic thin films the low energy features in the Fe K- and Mn K- edge polarization dependent XANES spectra increase with increasing DSRO of Fe and Mn, respectively. Building on the powerful combination of XANES experiment and simulation, we establish that the degree of DSRO of the specific element is proportional to the height of a low energy feature just above the absorption edge in case of Fe or Mn in  $L1_0$  FeMnPt magnetic thin films. Remarkably, subtle changes already show up in FeMnPt films for Mn doping from 10 at. % to 15 at. % in both Mn and Fe XANES spectra with the x-ray polarization parallel ( $E//\text{surface}$ ) and perpendicular ( $E\perp\text{surface}$ ) to the  $L1_0$  FePt (001) surface plane. Based on the DSRO results, a model of structural evolution as a function of Mn doping is proposed, which is also consistent with the observed LRO and magnetic properties. The qualitative investigation of DSRO by a combination of XANES analysis and the first-principle calculation developed in this study may provide a general method of study of DSRO in thin films measured with x-ray polarization parallel and perpendicular to the surface plane. This method may

also be extended to investigate the DSRO at any given lattice direction in other materials systems.

$\text{Fe}_{(50-x)}\text{Mn}_x\text{Pt}_{50}$  films (50 nm) with Mn concentrations of  $x=0$ , 10, and 15 at. % were deposited using sputtering onto single crystal MgO (100) substrates at 550 °C. The details of the sample fabrication and basic magnetic and structural properties were reported elsewhere [9]. In summary, all the films were epitaxially grown through the relation of MgO (001)  $\langle 100 \rangle$  //  $L1_0$  FePt (001)  $\langle 100 \rangle$ , and exhibit perpendicular magnetic anisotropy. The  $L1_0$  ordering parameter, perpendicular magnetic anisotropy, and saturation magnetization ( $M_s$ ) of the films decrease with the increasing of the atomic percentage of Mn doping. In particular, the sharp decrease of  $M_s$  with Mn doping was suggested to be associated with the formation of AFM  $L1_0$  MnPt phase.

The XANES measurements were performed using linear polarized x-rays at the undulator beamline 20-ID-B of the Advanced Photon Source (APS), Argonne National laboratory. Details on the beamline optics and instruments can be found elsewhere [10]. In particular, the microprobe station was used to provide a focused beams size of 3  $\mu\text{m}$ , allowing glancing angle measurements with x-ray polarization parallel and perpendicular to the (001) surface plane. Fe and Mn metal foils placed to intercept a scattered beam were used as an online check of the monochromator energy calibration [11]. The absorption edge positions for Fe and Mn were taken as 7110.75 eV and 6537.67 eV, respectively [12].

Due to the linear polarized x-ray, the x-ray absorption coefficient will show a polarization dependence for an anisotropic sample such as the L1<sub>0</sub> ordered FeMnPt films as illustrated in Equation-1 [7]

$$u(\theta) = u_{//} + (u_{\perp} - u_{//})\cos^2\theta \quad (1)$$

Where  $\theta$  is the angle between the polarization vector and surface normal,  $u_{//}$  and  $u_{\perp}$  are the absorption coefficient with polarization vector parallel or perpendicular to the surface of the sample. Further, the K and L<sub>1</sub> shells polarization factor  $p(e)$  that accounts for the polarization of the incoming x-rays can be written as [7]

$$p(e) = 3\cos^2\theta \quad (2)$$

If the materials have random orientations or have cubic or higher symmetry, then  $\cos^2\theta=1/3$  and  $p(e)=1$ . The absorption coefficient of powder-average spectra  $u_{isotropic}$ , which in this case assume the FeMnPt films are randomly oriented, can be written by substituting the  $\cos^2\theta=1/3$  in Equation 1 as follows

$$u_{isotropic} = \frac{2}{3}u_{//} + \frac{1}{3}u_{\perp} \quad (3)$$

In this study, the powder-average spectra, which are 1/3 of the perpendicular orientation signal plus 2/3 of the parallel orientation signal [7,13], of the films at the Fe and Mn K-edges are shown in Fig. 2a and Fig. 2c, respectively. The XANES of Fe metal foil has a low energy Shoulder-A near 7114 eV, a medium energy Shoulder-B near 7121 eV, and a high energy Peak-C at 7129 eV; the XANES of Mn metal foil gives rise to a low energy Shoulder-A near 6540 eV and a high energy Peak-C at 6555 eV. The low energy Shoulder-A

can be assigned to a p-projected density of states hybridized with the 3d-states of the surrounding atoms [14,15]. Figures 2b and d show the first derivative of the Fe and Mn absorption edges. Peak E is used to define the absorption edge energy, and peak F defines the position of the low energy Shoulder-A. The heights of low energy Shoulder-A at both the Fe K-edge (Figs. 2a) and the Mn K-edge (Fig. 2c) increase when the respective element composition increases in the thin films. Assuming the Fe and Mn is uniformly distributed in the epitaxial-grown thin films, the increase of Fe or Mn composition is associated with an increasing fraction of Fe-Fe and Mn-Mn bonds; thus, the height of the low energy shoulder at the Fe K- or Mn K- edge can be related to the degree of SRO in the Fe-Fe or Mn-Mn bonding.

Why does the height of the low energy shoulder at the Fe K- or Mn K-edge increase when the SRO of Fe-Fe or Mn-Mn is increased? The increase of the height of a similar low energy shoulder with the increase of its corresponding elemental composition has been found in various cases. For example, the heights of the low energy shoulders of Fe and Ni decrease when the compositions of Fe and Ni are reduced in FeNi alloys [14], the height of a low energy shoulder of Cu increases as the Cu composition is increased in the CuPt [16] and CuAu [17] alloys, the height of the low energy shoulder of Fe declines when the thickness of Fe in a  $[\text{Fe}/\text{Si}_3\text{N}_4]_n$  multilayer is decreased [18]. Although a complete interpretation of the correlation between the height of the low energy shoulder and the constituting elemental composition is still lacking, these examples reflect the mounting evidence that the height of a low energy shoulder might be proportional to the SRO for the 3d transition metals. As pointed out above, the low energy shoulder is associated with a p-

projected density of states hybridized with the 3d-states of the surrounding atoms [14,15], the increase of the SRO of Fe-Fe or Mn-Mn would result in a decrease of the hybridization, giving rise to an increase of unoccupied states. Therefore, the height of the low energy shoulder becomes more pronounced.

Is the height of low energy shoulder of the polarization dependent XANES proportional to the DSRO of the element of interest? To answer this, both polarization dependent XANES experiment and simulation were employed to study the correlation of DSRO and the height of the low energy shoulder at its absorption edge.

The XANES spectra with the x-ray polarization parallel and perpendicular to the  $L1_0$  FePt (001) lattice plane were calculated using *ab initio* Feff8.4 code [19]. Specifically, a cluster of 103 atoms with size of 7 Å was applied for the calculation of full-multiple scattering (FMS), a cluster of 55 atoms with size of 5.5 Å was used for the calculation of the self-consistent-field (SCF) muffin-tin atomic potential, and a Hedin-Lundqvist exchange potential of 2.0 eV was chosen to account for the broadening of the spectra.

Figure 3 displays the calculated Fe K-edge (a) and Mn K-edge (b) XANES both parallel and perpendicular to the  $L1_0$  FePt (001) plane. The isotropic spectrum for unpolarized x-rays is also shown as reference. The lattice parameters of  $L1_0$  Fe<sub>50</sub>Pt<sub>50</sub> films in this study were applied in the calculation for both Fe K-edge and Mn K-edge. The calculated XANES spectra at both the Fe K-edge (Fig. 3a) and Mn K-edge (Fig. 3b) indicate a significant polarization dependence; the height of the low energy shoulder of the parallel spectrum is higher than that of the perpendicular one, with the

isotropic spectrum in between. For an ideal  $L1_0$  ordered phase there is complete directional short range order, and the signal of parallel XANES mainly results from the Fe-Fe bonds in the (001) plane, whereas the perpendicular XANES is caused by a combination of Fe-Pt and Fe-Fe bonds in the [001] direction. The isotropic spectrum consists of 1/3 of the perpendicular orientation signal plus 2/3 of the parallel orientation signal. The sequence of the degree of DSRO of Fe from high to low is parallel to (001) plane, the isotropic, and perpendicular to (001) plane, which is the sequence of the height of the low energy shoulders for the simulated spectra (Fig. 3a). A similar result is found from the XANES calculation of the polarization dependent  $L1_0$  MnPt ordered phase. The XANES calculations for both  $L1_0$  FePt (Fig. 3a) and  $L1_0$  MnPt (Fig. 3b) phases indicate that the height of the low energy shoulder of the polarization dependent XANES is proportional to the degree of DSRO of the element of interest in case of  $L1_0$  FePt and MnPt systems. Furthermore, our calculations of polarization dependent XANES spectra for the  $L1_0$  ordered phase are also consistent with other XANES calculations for the  $L1_0$  ordered FePt [20] and CoPt [21] phases. By comparing the earlier work with our calculation, similarities can be found in both the shape and the height of the low energy shoulder, but the DSRO was not specifically discussed in these studies [20,21].

Figure 4 displays the polarization dependent XANES measurements for the FeMnPt films at both the Fe (Fig. 4a) and Mn K-edges (Fig. 4b), respectively. The heights of the low energy Shoulder-A and difference in the low energy Shoulder-A between parallel and perpendicular XANES measurements are shown in Fig. 4c and Fig. 4d. While the error bars in the

heights of the features for the Mn K-edge and their differences are relatively large, the results suggest that the trend of differences of DSRO in Mn as a function of Mn composition follows that of Fe, indicating that the Mn is substituting into Fe sites in the FePt films. Remarkably, subtle changes already show up in FeMnPt films when the Mn doping increases from 10 at. % to 15 at. % for both the Mn and Fe XANES spectra. Comparing the DSRO of Mn in the  $\text{Fe}_{40}\text{Mn}_{10}\text{Pt}_{50}$  and  $\text{Fe}_{35}\text{Mn}_{15}\text{Pt}_{50}$  films, the difference of DSRO for Mn at  $\text{Fe}_{40}\text{Mn}_{10}\text{Pt}_{50}$  films is larger than that of  $\text{Fe}_{35}\text{Mn}_{15}\text{Pt}_{50}$ , though the Mn doping is lower in the  $\text{Fe}_{40}\text{Mn}_{10}\text{Pt}_{50}$  films compared to that of  $\text{Fe}_{35}\text{Mn}_{15}\text{Pt}_{50}$  films. These observed DSRO (Fig. 4) are consistent with a decrease of ordering parameter with increasing Mn doping [9]. In addition, the finding that  $\text{DSRO}_{\perp}$  of Fe is constant as a function of the Mn content can be understood as follows: when the Mn content increases, the  $L1_0$  ordering decreases; on one hand, the decreasing of  $L1_0$  ordering increases the  $\text{DSRO}_{\perp}$  of Fe, on the other hand, the increasing of Mn content decreases of the  $\text{DSRO}_{\perp}$  of Fe as a result of the decreasing of the total Fe content in the films, consequently, the  $\text{DSRO}_{\perp}$  of Fe can be constant as a function of the Mn content due to the combined effects. In a separate study of the polarization dependence of the XANES spectra of an Fe layer on the GaAs surface [22], the low energy shoulder reduces in both parallel and perpendicular directions when the number of Fe monolayers is decreased. As reducing the number of Fe monolayers results in the decrease of the DSRO of Fe in both directions, the observation of decreasing of low energy shoulder with decreasing thickness of the Fe monolayer can be understood as due to a decrease of the DSRO of Fe in both directions, offering solid experimental support for this study. The combination of

theoretical calculations of XANES spectra (Fig. 3), and polarization dependent XANES measurements (Fig. 4) suggests that the low energy shoulder could be used to study the DSRO of the element of interest in case of Fe or Mn in  $L1_0$  FeMnPt magnetic thin films.

The observed magnetic properties of the FeMnPt films and the  $L1_0$  ordering, obtained from LRO characterization as a function of Mn composition in this work [9], also verify the DSRO of Fe and Mn obtained by the polarization dependent XANES experiments and calculations. As discussed above, the most stable phase for  $L1_0$  MnPt is an AFM phase with AFM ordering in the (001) plane, and FM order between the (001) planes (Fig. 1).  $L1_0$  FePt is a FM phase with the stable status of all spins aligning perpendicular to the (001) direction (Fig. 1). Based on the DSRO analysis, the structural evolution as a function of Mn doping is suggested as follows: Mn is substituting into the Fe site in  $L1_0$  FeMnPt films, the DSRO of Mn follows the DSRO of Fe; the difference of DSRO of both Fe and Mn decreases as the Mn doping increases, however the absolute amount of parallel DSRO of Mn within (001) lattice plane in  $Fe_{35}Mn_{15}Pt_{50}$  is much higher than that of Mn in  $Fe_{40}Mn_{10}Pt_{50}$  (Fig. 4c). As shown in Fig. 1, the magnetic spin of Mn atom prefers to align antiferromagnetically with the magnetic spin of neighboring Mn atoms within the (001) lattice plane to minimize the total energy, thus forming AFM phase [5]. Accordingly, the accumulation of AFM phase in the (001) plane when the Mn doping is increased leads to a sharp decrease of  $M_s$  [9].

In summary, a new method is described, which investigates the DSRO of an element of interest using polarization dependent XANES spectroscopy. We demonstrate theoretically and experimentally that the height of the low

energy shoulder in the K-edge polarization dependent XANES in case of Fe or Mn in  $L1_0$  FeMnPt magnetic thin films is proportional to the DSRO of the element of interest.

**Acknowledgements:**

PNC/XSD facilities at the Advanced Photon Source, and research at these facilities, are supported by the US Department of Energy - Basic Energy Sciences, a Major Resources Support grant from NSERC, the University of Washington, Simon Fraser University and the Advanced Photon Source. Use of the Advanced Photon Source, an Office of Science User Facility operated for the U.S. Department of Energy (DOE) Office of Science by Argonne National Laboratory, was supported by the U.S. DOE under Contract No. DE-AC02-06CH11357. This work is partially supported by Ministry of Education, Singapore under grant No. R-284-000-061-112, and A\*STAR under grant R-284-000-082-305.

## References:

- [1] S. S. A. Razee, J. B. Staunton, B. Ginatempo, F. J. Pinski, and E. Bruno, *Phys. Rev. Lett.* 82, 5369 (1999).
- [2] J. C. Loudon, N. D. Mathur, and P. A. Midgley, *Nature* 420, 797 (2002).
- [3] H. Bernas, J. P. Attane, K. H. Heinig, D. Halley, D. Ravelosona, A. Marty, P. Auric, C. Chappert, and Y. Samson, *Phys. Rev. Lett.* 91, 077203 (2003).
- [4] G. Meyer and J.-U. Thiele, *Phys. Rev. B* 73, 214438 (2006).
- [5] Z. H. Lu, R. V. Chepulsii, W. H. Butler, *Phys. Rev. B* 81, 094437 (2010).
- [6] S.-W. Han, E. A. Stern, D. Haskel, and A. R. Moodenbaugh, *Phys. Rev. B* 66, 094101 (2002).
- [7] S. M. Heald and E. A. Stern, *Phys. Rev. B* 16, 5549 (1977); and S. M. Heald, XAFS spectroscopy, in *Characterization of Materials*, edited by E. N. Kaufmann, (Hoboken, N.J.: Wiley-Interscience, c2003), p 873.
- [8] G. M. Chow, W. C. Goh, Y. K. Hwu, T. S. Cho, J. H. Je, H. H. Lee, H. C. Kang, D. Y. Noh, C. K. Lin, and W. D. Chang, *Appl. Phys. Lett.* 75, 2503 (1999).
- [9] D. B. Xu, J. S. Chen, T. J. Zhou, and G. M. Chow, *J. Appl. Phys.* 109,07B747 (2011).
- [10] S. M. Heald, J. O. Cross, D. L. Brewes, and R. A. Gordon, *Nucl. Instrum. Methods Phys. Res. A* 582, 215 (2007).
- [11] J. O. Cross and A. I. Frenkel, *Rev. Sci. Instrum.* 70, 38 (1999).
- [12] S. Kraft, J. Stumpel, P. Becker, and U. Kuetgens, *Rev. Sci. Instrum.* 67, 681 (1996).

- [13] S. M. Heald, T. C. Kaspar, T. Droubay, V. Shutthanandan, S. A. Chambers, A. Mokhtari, A. J. Behan, H. J. Blythe, J. R. Neal, A. M. Fox, and G. A. Gehring, *Phys. Rev. B* 79, 075202 (2009).
- [14] H. Sakurai, F. Ito, H. Maruyama, A. Koizumi, K. Kobayashi, H. Yamazaki, Y. Tanji, and H. Kawata, *J. Phys. Soc. Jpn.* 62, 459 (1993).
- [15] J. E. Müller, O. Jepsen, and J. W. Wilkins, *Solid State Commun.* 42, 365 (1982).
- [16] Y.-S. Lee, K.-Y. Lim, Y.-D. Chung, C.-N. Whang, and Y. Jeon, *Surf. Interface Anal.* 30, 475 (2000).
- [17] M. Kuhn, T.K. Sham, J.M. Chen, and K.H. Tan, *Solid State Commun.* 75, 861 (1990).
- [18] F. Jiménez-Villacorta, E. Céspedes, M. Vila, A. Muñoz-Martín, G. R. Castro, and C. Prieto, *J. Phys. D: Appl. Phys.* 41, 205009 (2008).
- [19] A.L. Ankudinov, A.I. Nesvizhskii, and J.J. Rehr, *Phys. Rev. B* 67, 115120 (2003).
- [20] A. Martins, N. M. Souza-Neto, M. C. A. Fantini, A. D. Santos, R. J. Prado, and A. Y. Ramos, *J. Appl. Phys.* 100, 013905 (2006).
- [21] N. M. Souza-Neto, A. Y. Ramos, Hélio C. N. Tolentino, A. Martins, and A. D. Santos, *Appl. Phys. Lett.* 89, 111910 (2006).
- [22] R. A. Gordon, E. D. Crozier, D.-T. Jiang, P. S. Budnik, T. L. Monchesky, and B. Heinrich, *Surf. Sci.* 581, 47 (2005).

### Figure Captions:

Figure 1. Models of  $L1_0$  ordered FePt or MnPt alloy. a, A ferromagnetic (FM) type  $L1_0$  ordered alloy. b, An antiferromagnetic (AFM) type  $L1_0$  ordered alloy. c, The big blue filled circles are Pt atoms, and the small purple filled circles are Fe or Mn atoms. d, The lattice directions of the  $L1_0$  structure. The details of the models are discussed in Ref. 5.

Figure 2. Measured XANES spectra, consisting of 1/3 of the perpendicular orientation signal plus 2/3 of the parallel orientation signal. a, XANES spectra at the Fe K-edge for Fe metal and FeMnPt films, the difference between the  $Fe_{40}Mn_{10}Pt_{50}$  and  $Fe_{35}Mn_{15}Pt_{50}$  can be found at the inset of the Fig.2a. b, The derivative of XANES spectrum of Fe metal foil. c, XANES spectra at the Mn K-edge for Mn metal and FeMnPt films. d, The derivative of XANES spectrum of Mn metal foil. A, B, and C in Fig. 2a and Fig. 2c denote the low energy shoulder, and medium energy shoulder, and high energy peak. E and F in Fig. 2b and 2d correspond to the absorption edge and the first negative peak.

Figure 3. Calculated XANES spectra. a, The calculated polarization dependent XANES spectra of  $L1_0$   $Fe_{50}Pt_{50}$  using *ab initio* Feff8.4 code at the Fe K-edge. b, The calculated polarization dependent XANES spectra of  $L1_0$   $Mn_{50}Pt_{50}$  using *ab initio* Feff8.4 at the Mn K-edge. The isotropic XANES spectra without polarization dependence are displayed as reference.

Figure 4 Measured polarization dependent XANES spectra. a, Polarization dependent XANES spectra of FeMnPt films at the Fe K-edge. Five separate measurements are used to obtain the averaged Fe XANES. b, Measured polarization dependent XANES spectra of FeMnPt films at the Mn

K-edge. Four separate measurements are used to obtain the averaged Mn XANES. c, The intensity of low energy shoulders as a function of the Mn composition. The error bars were obtained by comparing the averaged XANES with the individual scans. d, The difference DSRO ( $DSRO_{//}-DSRO_{\perp}$ ) of Fe and Mn as a function of the Mn composition.

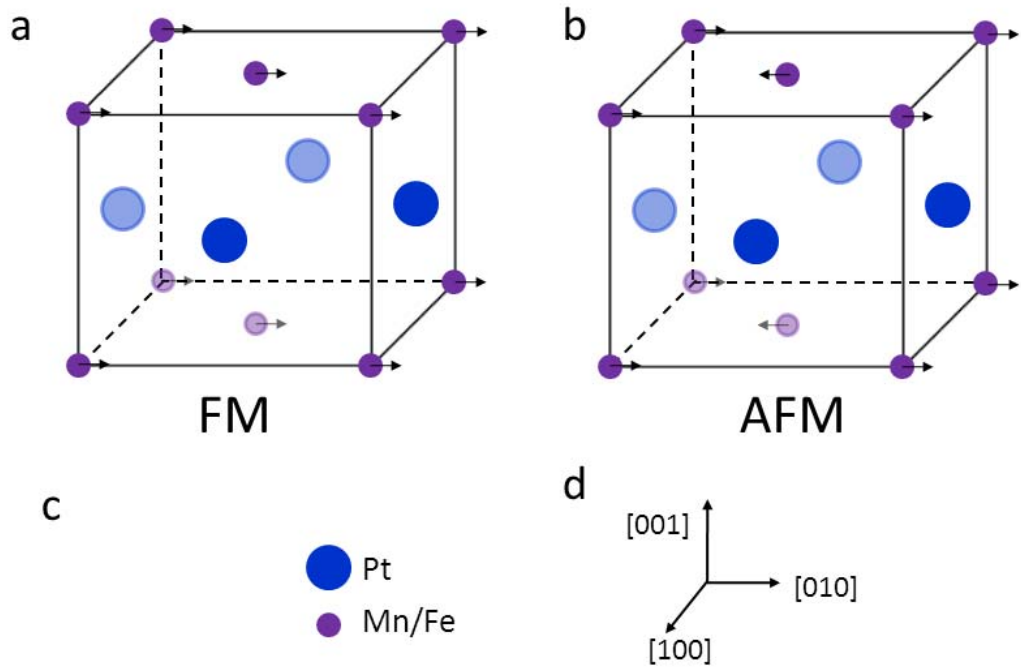


Figure1. Cheng-Jun Sun et al., submitted to PRB

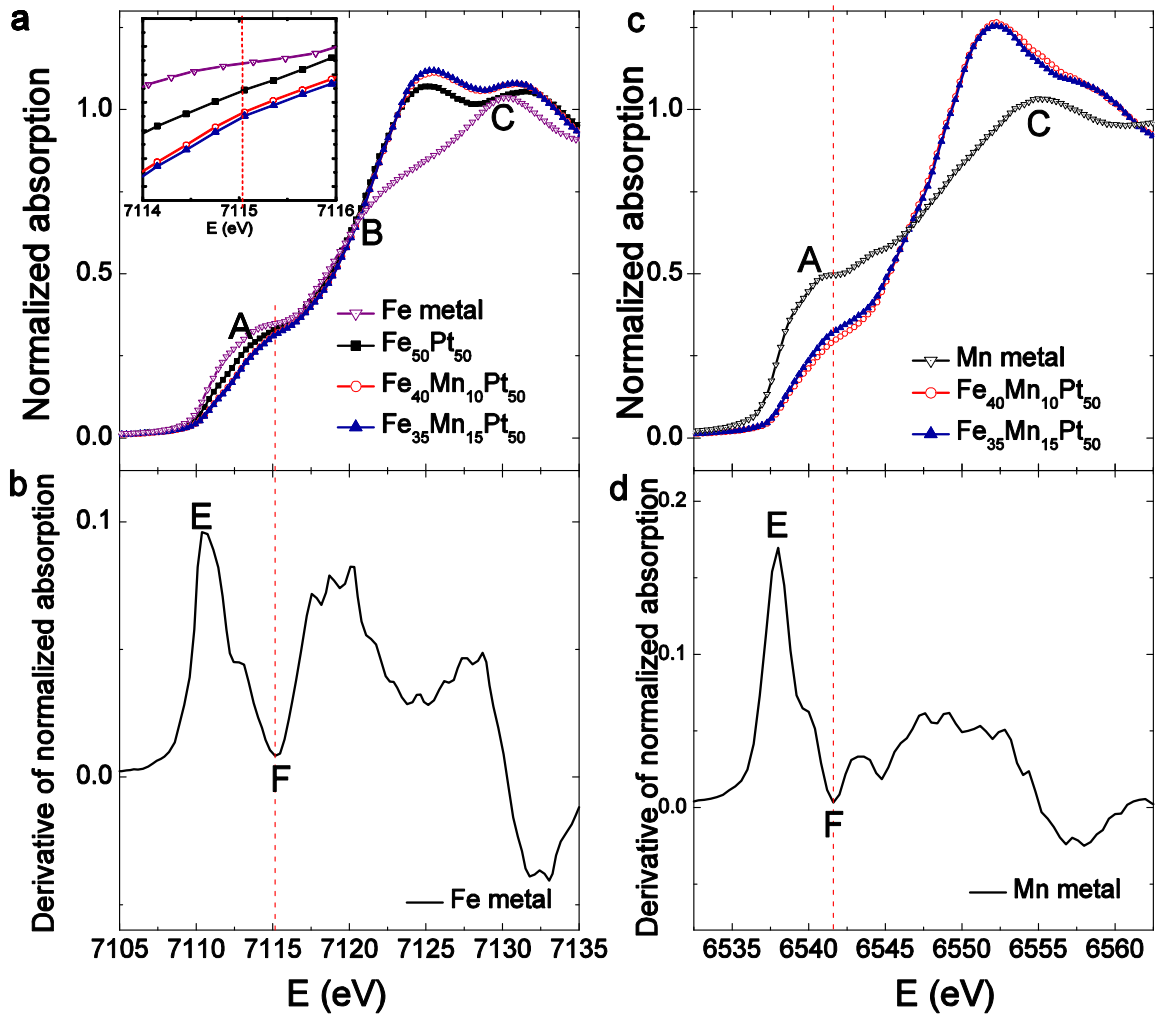


Figure 2. Cheng-Jun Sun et al., submitted to PRB

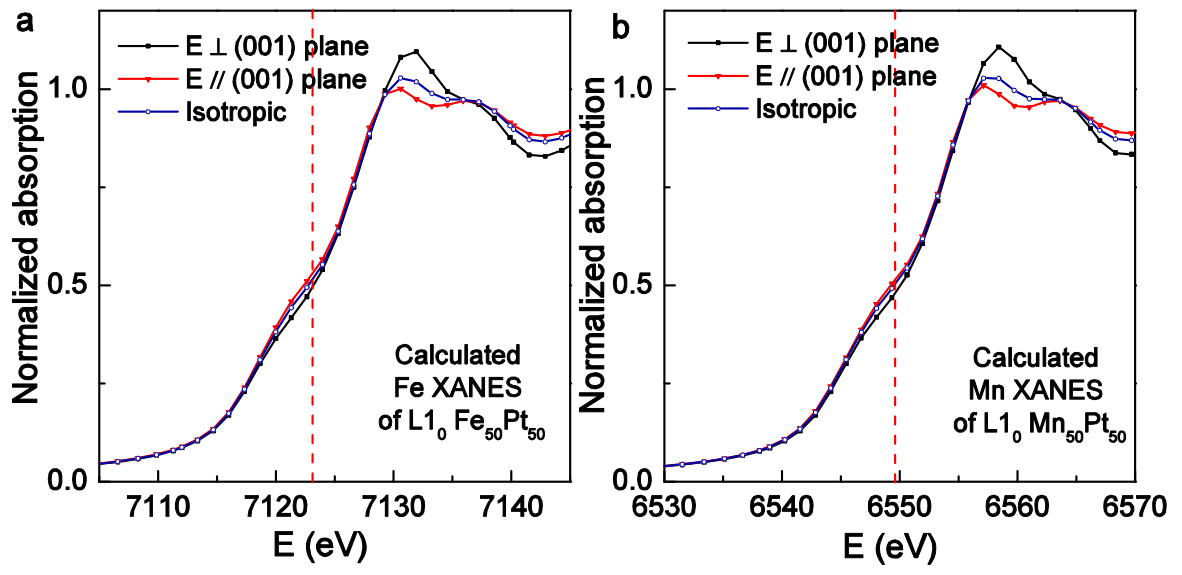


Figure 3. Cheng-Jun Sun et al., submitted to PRB

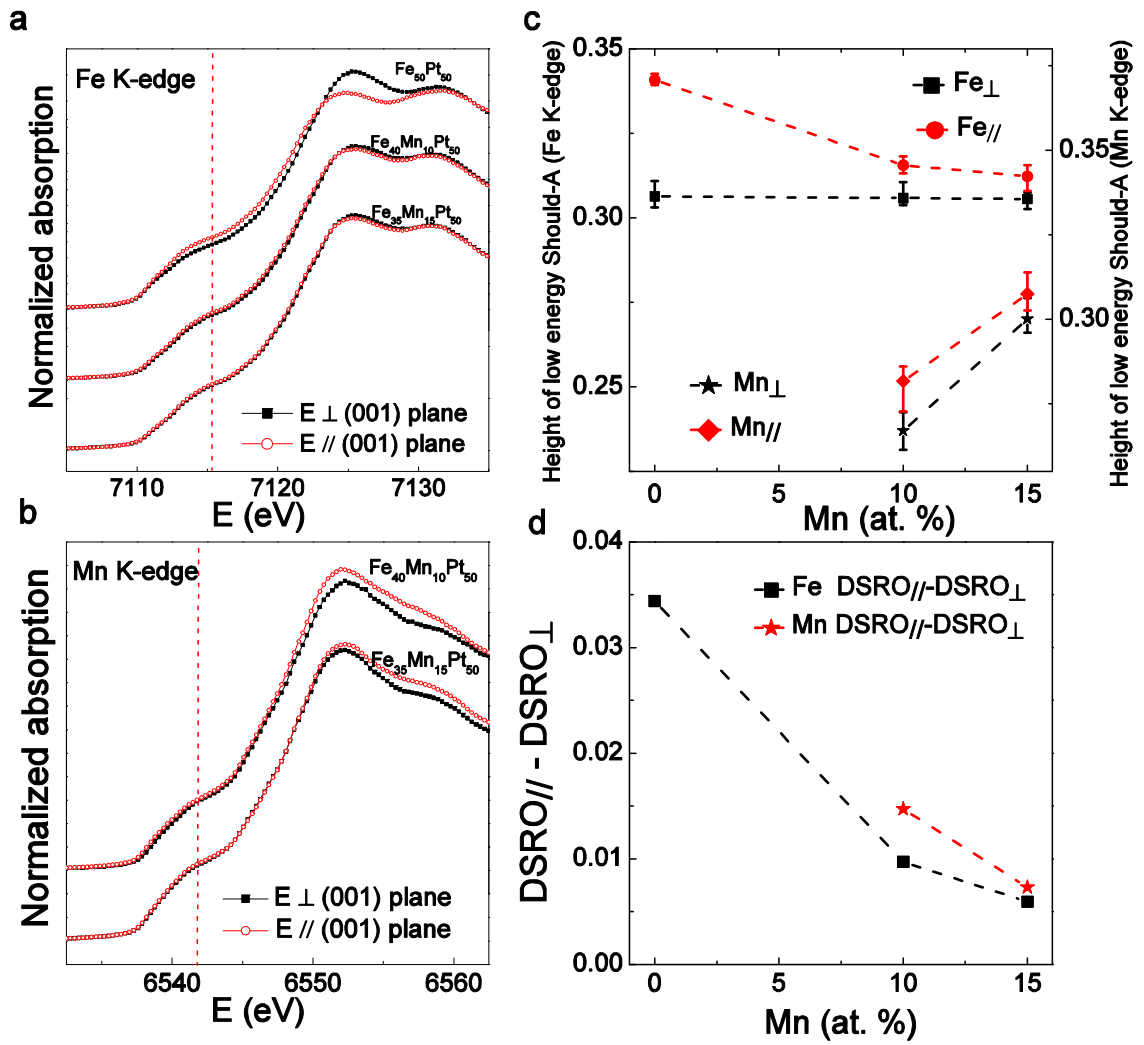


Figure 4. Cheng-Jun Sun et al., submitted to PRB